39

APPLICATION OF A BLENDED MW-IR RAINFALL ALGORITHM TO THE MEDITERRANEAN

Francesca Torricella[1],Vincenzo Levizzani[1], and F. Joseph Turk[2]
[1]*Institute of Atmospheric Sciences and Climate, ISAC-CNR, Bologna, Italy*
[2]*Naval Research Laboratory, NRL, Monterey, CA, USA*

1 INTRODUCTION

The network of meteorological and environmental satellites is the only practicable means of monitoring and gauging rainfall on a global scale. For this reason an adequate estimation of the accuracy of global operational rain products is crucial. The first step for estimating error characteristics is perhaps a kind of *local* analysis, validation campaign and limited comparisons with reference data sets, in general taken from ground based instruments and networks, deemed to represent "truth" data sets. Historically, ground based radar and rain gauges supplied the reference data for such comparisons. With the advent of space based radars such as the precipitation radar of the Tropical Rainfall Measurement Mission (TRMM) reference data sets are also available from space. Moreover, the comparison with products derived from concurrent sensors (e.g., TRMM mixed radar-microwave products) is is another tool to check the overall performance of newly developed algorithms. A parallel approach consists in developing an error model of the retrieval process and assessing the uncertainties of its parameters. The key here is that the product being validated be derived on a physical basis with empirically verifiable assumptions. To date, the largest efforts of the scientific community have been aimed to the assessment of the accuracy of mean (monthly, weekly, daily) or cumulated rain products over suitable study periods and using standard evaluation statistics (Adler et al. 2001). Nevertheless, the application of satellite derived analysis to the characterization of severe rain events, meteorological applications, and flood management requires that the global achievements of the validation exercise

V. Levizzani et al. (eds.), Measuring Precipitation from Space: EURAINSAT and the Future, 497–507.

be verified on a local scale. It is necessary to understand whether useful and reliable estimates of precipitation fields can be obtained in particular climatic and geographic conditions. The goal is to analyze the performances of the method in producing instantaneous rainfall maps. It is conceivable that global algorithms need local optimization if snapshots of the precipitation field are required for the devised applications, because the physics of the rain processes strongly depends on the immediate environment.

A global blended infrared-passive microwave (IR-PMW) technique producing rain rate fields at the time/space resolution and coverage of geo-stationary (GEO) observations is applied to rain events over Mediterranean countries. Two cases are examined: a series of intense rainstorms that affected the Emilia-Romagna area (Northern Italy) in early August 2002, and the November 2001 Algeria flood. In spite of their unusual intensity, they were selected among a set of analogous cases for they are representative of several common characteristics that a rain algorithm should be capable of coping with when functioning in such particular environment.

2 THE HYBRID PMW-IR RAINFALL ESTIMATION METHOD

The idea of using data from GEO satellites to produce rain rate (RR) maps over large areas of the globe was largely exploited using visible (VIS) and IR stand-alone observations or combining them with information from different sensors, especially PMW instruments on polar platforms. At present, only GEO measurements have the spatial resolution (a few km^2), repetition time (15–30 min), and spatial coverage suitable to properly follow the rapid variations of precipitation fields. Moreover, the long history and the robust technology of GEO instruments prompts for the reanalysis of historical events and guarantees a timely and reliable release of calibrated data. VIS and IR measurements give only indirect information on the precipitation field being limited to the uppermost cloud layer near the top. Their uncertainties are thus relevant *per se* since the precipitating hydro-meteors do not interact directly with the photons collected aloft by space borne instruments at these wavelengths. Several methods have been developed that “calibrate” for example IR brightness temperature (T_B) data by using the more physically based rain estimates derived from PMW instruments. This kind of blended techniques is intrinsically constantly evolving due to the ever-expanding suite of PMW sensors and multispectral GEO imagers. Moreover they should mitigate the sampling error deriving from non-continuous precipitation sampling due to the orbital characteristics of the satellite and the spatio-temporal structure of precipitation associated with diurnal, synoptic, seasonal, and interannual variability cycles.

The blended technique adopted hereafter (Turk et al. 2000b) has been recently validated using rain-gauge data and analyses by the Korean Meteorological Agency and the Australian Bureau of Meteorology. Looking at mean or cumulated rainfall amounts, the correlation fairly increases and bias and root mean square error decreases as either the integration/averaging period is increased (from a minimum of 1 h up to 30 days) or the grid size for spatial averaging is coarsened (from 0.1 to 3°). The original operational set up of the software (global, automatic, real time, using a suite of PMW and IR observations) was adapted to the task of analyzing test case studies. In the Turk's method, hereafter referred to as Naval Research Laboratory technique (NRLT), rain rates derived from PMW measurements are used to create global, geolocated RR-T_B relationships that are renewed as soon as new collocated data are available from both GEO and PMW instruments. The PMW RR data can be derived, in principle, from any source, provided they are geolocated rain intensities in mm h^{-1}, and that the files containing them report the useful information on orbit (date, start time, sensor, satellite, etc.). For the present work the adopted PMW estimates are mainly derived from Special Sensor Microwave/Imager (SSM/I) data. From the brightness temperatures measured in seven polarized channels from 19.2 to 85.5 GHz, rain rates are derived by means of the NOAA-NESDIS operational algorithm (Ferraro and Marks 1995; Ferraro 1997). The NESDIS algorithm derives rainrates at the A-scan resolution of the SSM/I (~25 km) by means of nonlinear relationships involving the instrument channels (vertical and horizontal polarization) that have been calibrated using large sets of ground reference data collected by radar networks in different countries. The physical basis of such relationships are the scattering of MW radiation due to large ice particles above the freezing level occurring in precipitating clouds, and the emission from liquid water. This latter phenomenon can be sensed only above oceanic surfaces, due to high and largely unknown emissivity of land surfaces in the MW spectral range. Relying on PMW measurements only (no need of large input database of physical properties) and on simple but well founded relationships, this algorithm is very robust and lends itself to global applications. In the NRLT, to the end of calibrating IR measurements, the globe (or the study area) is subdivided in equally spaced LAT-LON boxes (2.5° × 2.5°). For each box, space and time coincident IR and PMW measurements are reduced to the worse spatial resolution and then collected. The colocation process allows for time and space offsets (15 min and 10 km, respectively). To form a meaningful statistical ensemble the method can look at older PMW orbit-IR slot intersections, until a certain box coverage is reached (say 75%) and a minimum number of coincident observations is gathered for a 3° × 3° boxes region. By means of this set of RR and corresponding T_B, the RR-T_B relationships are derived by applying a probability matching method (Calheiros and Zawadzki 1987).

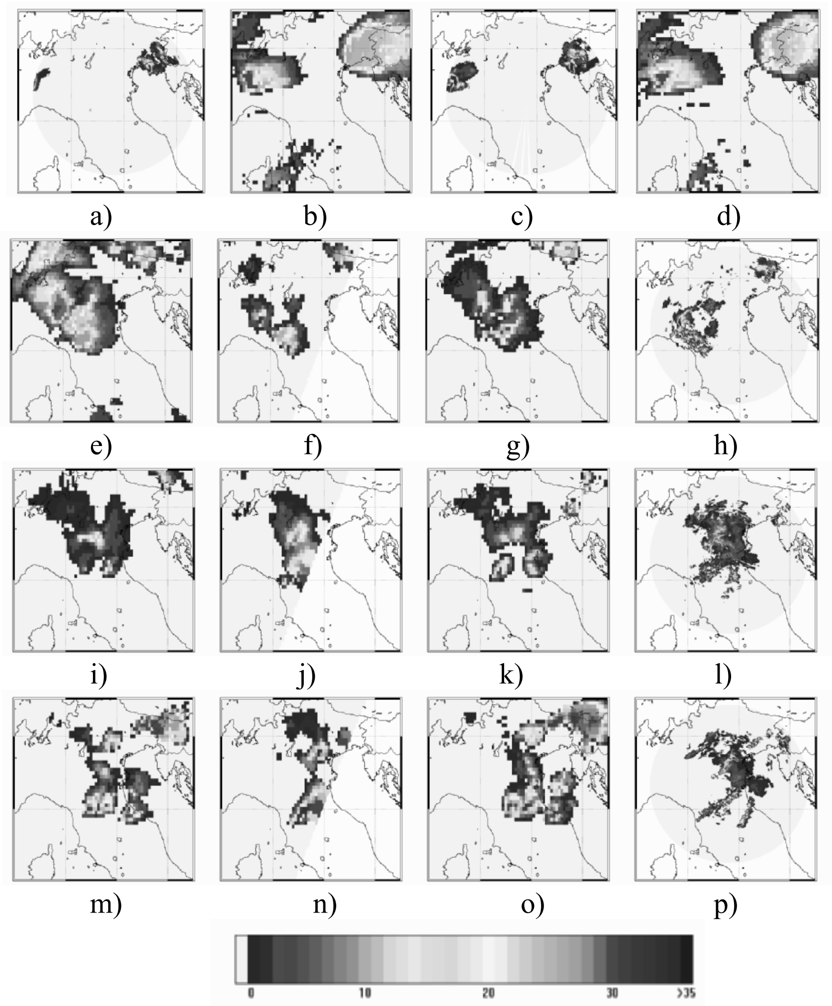

Figure 1. 6 August, 2002. Rain intensity maps in mm h^{-1} for the Emilia-Romagna storm case study. All times are UTC. a) Radar map at 0012; b) NRLT for the slot starting at 0000; c) Radar map at 0042; d) NRLT for the slot starting at 0030; e) NRLT for the slot starting at 0630; f) PMW NESDIS algorithm for the SSM/I orbit 08D (F13) starting at 0627; g) NRLT for the slot starting at 0700; h) Radar map at 0642; i) NRLT for the slot starting at 0800; j) PMW NESDIS algorithm for the SSM/I orbit 10D (F14) starting at 0828; k) NRLT for the slot starting at 0800; l) Radar map at 0842; m) NRLT for the slot starting at 0930; n) PMW NESDIS algorithm for the SSM/I orbit 12D (F15) starting at 0941; o) NRLT for the slot starting at 1000; p) Radar map at 0942. (see also color plate 17)

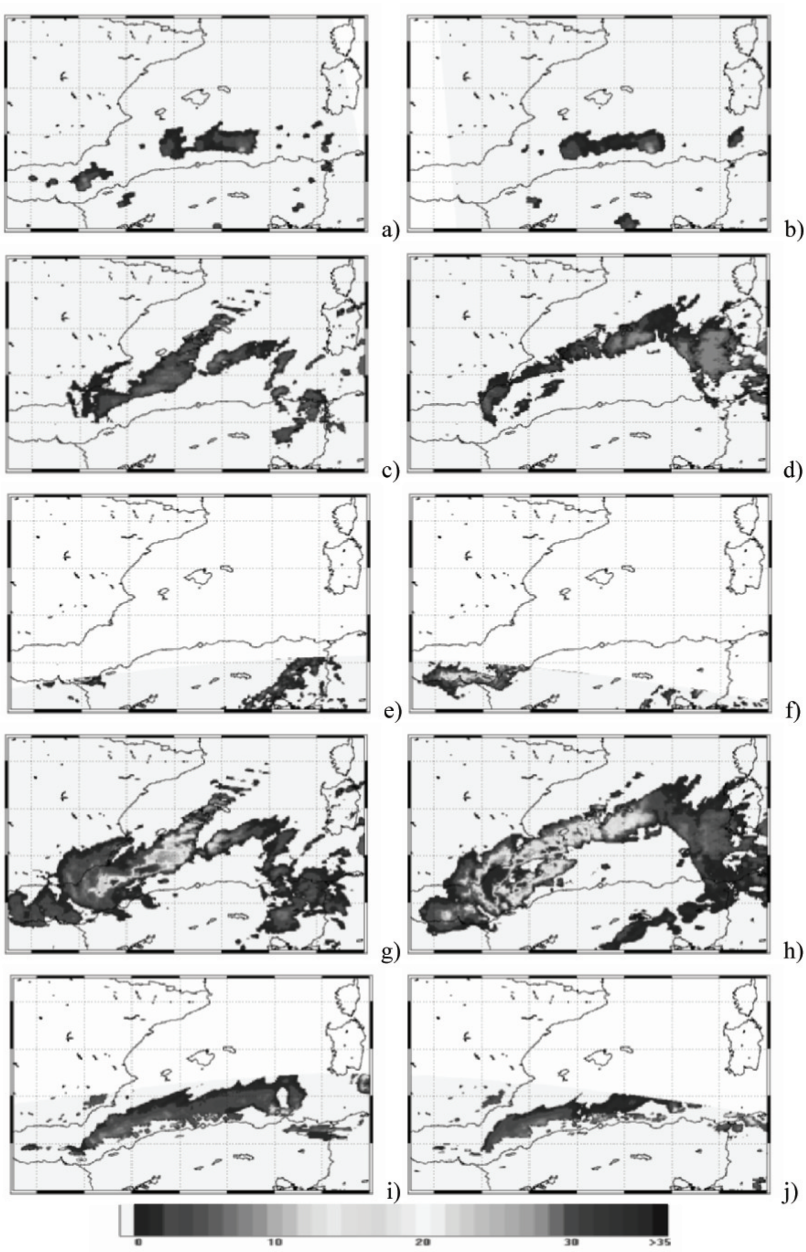

Figure 2. 10 November, 2001. Rain intensity maps in mm h^{-1} for the Algeria case study. Time is UTC. a) SSM/I orbit 23A (F14) starting at 1919; b) SSM/I orbit 24A (F15) starting at 1958; c) NRLT for the slot starting at 0000; d) NRLT for the slot starting at 0200; e) PR for the TRMM orbit 22741 (area overpass around 0032); f) PR for TRMM orbit 22742 (area overpass around 0210); g) NRLT for the slot starting at 0000 (calibrated with PR data); h) NRLT for the slot starting at 0200 (calibrated with PR); i) 2A12 TMI rainrates for the TRMM orbit 22741; j) 2A12 TMI rainrates for the TRMM orbit 22742.

3 AUGUST 2002 INTENSE RAINSTORMS OVER EMILIA-ROMAGNA

The Po Valley in Northern Italy is surrounded on three sides by high mountains and is therefore characterized by relatively high humidity and light winds at lower atmospheric levels, rather favorable conditions for the formation of line storms and Mesoscale Convective Systems. In August 2002 a number of intense storms hit the Italian peninsula, and attained a relevant intensity over a large area from Tuscany through Emilia-Romagna all the way up to northeastern Italy. Hailfall damages were widely registered in the belt between France, Switzerland, southern Germany, Austria, Hungary, and the Caucasus region.

Early in the month instability conditions were fostered by a cyclonic area insisting over France, with cold air fluxes over north-central Italy, with associated strong winds, heavy rainfall, and hailstorms. The monthly rainfall accumulations reached unusually high values, with a maximum positive anomaly of 100 mm in Ferrara. Rainstorms started on the 4th and, after a few hours of pause, they intensified again in the afternoon of the 5th one after the other with similar characteristics and hitting a limited geographical area. The storm cells originated west of the Alps and moved rapidly eastward crossing the entire Po Valley. The electric activity remained quite impressive during the entire duration.

The first useful SSM/I overflight is the orbit at 1601 UTC on day 5. Later on, the zone was imaged 6 times by the SSM/I sensors in about 24 h, thanks to the availability of data from three satellites (F13, F14, and F15). The starting time of the orbits on day 5 were 1601, 1802 and 1916 UTC, and there was no overpass during the night. The first overpass on day 6 corresponds to the orbit starting at 0627 UTC and the area was then covered by the orbits 0828, 0941 and 1547 UTC. After 1600 UTC the storm system left the region and moving eastward toward Slovenia.

The rain maps for the overpass on day 6 are shown in Fig. 1. On the overall, the PMW algorithm detects the storm cells and gauges the high precipitation intensities up to 35 mm h^{-1}, the maximum allowed rain intensity in the NESDIS algorithm (panels f, j, n). Note that all the SSM/I orbits cover the western part of the area (the gray shad delimits the area where the method/instrument gives results). The first row in the figure collects the results from NRLT for two slots during the night (panels b and d). For comparison nearly simultaneous radar maps are shown (panels a and c). Radar data are taken from C-band dual polarisation Doppler weather radar of the Servizio Meteorologico Regionale (SMR) in S. Pietro Capofiume, (44.654° N, 11.624° E, 11 m a.s.l.) in the southeastern sector of the Po valley. For these two slots, the last PMW overpass that calibrated the relationships for the blended rain intensities was the one on day 5 starting at 1916

UTC, i.e., it was about 3 h old. This can be perceived by observing the precipitation cell over the Italy-Slovenia border. The NRLT correctly followed the movement of this cell, but the precipitation field became unrealistically extended, somewhat uniform, and the peak intensity was too low. Nonetheless, the NRLT located the new cell in the west, with peak intensity, location and shape in good agreement with radar measurements. This rather good performance is confirmed by looking at the NRLT map (panel e) just before the next PMW calibration (panel f) in early morning of day 6. The location of the rain cells is still preserved more than 11 h after the last calibration, and the rain field matches closely the radar data (panel h). The agreement obviously improves in picture g, due to the intervening PMW calibration (panel f).

The capability of NRLT in extending the rain field information outside the PMW spatial coverage is testified in the next row of Fig. 1. The easternmost cell detected by radar in panel l (over Istria) is revealed also by NRLT even if no direct PMW measurements was available for this area since many hours. The last row in Fig. 1 (panels m, n, o, and p) confirms the NRLT performances with the exception of the feature in the upper-right corner of panel o that appears to be structureless.

4 THE NOVEMBER 2001 ALGERIAN FLOOD

In early November 2001, a widespread frontal system and upper air trough from northeast Scandinavia to southwest Spain led to an extreme precipitation event in Algiers, causing severe flooding and huge mudslides. More than 120 mm of rain fell in 12 h during the night between 9 and 10 November and more than 130 mm during the next 6 h on the mountains behind Algiers. The unusually large rain rates were fed by the cold maritime arctic air that picked up moisture crossing the warm Mediterranean waters and met maritime subtropical air. An intense orographic enhancement was caused by strong surface winds oriented towards the high mountains of the African coast (>2300 m a.s.l.).

The sudden onset of precipitation, the orographic complexity of the terrain, the vicinity to the coast are all elements that can introduce large errors and bias in PMW rainfall retrieval algorithms. Due to the short duration of the event (about 20 h), the area was imaged only a few times by PMW instruments. In such unfavorable condition, rapid update techniques are a powerful instrument to follow the evolution of the otherwise poorly observed rain field. The scarcity of validation data suggested a strategy involving not only SSM/I data but also data from the instruments onboard the Tropical Rainfall Measuring Mission (TRMM). The SSM/I derived RR fields were used for the calibration of the statistical relationships within the NRLT while the TRMM Microwave Imager (TMI) 2A12 operational rain product was retained as a source of comparison/validation data. Moreover, due to the unsatisfactory results of the NESDIS SSM/I rain algorithm, the NRLT was re-applied using measurements of the TRMM Precipitation Radar (PR) (2A25 operational product) as a calibration source for the blended product.

The rain maps for the central hours of the night between 9 and 10 November are collectively shown in Fig. 2 and document the peak intensity of the event. Note the following features for interpreting the rain maps: (a) the gray shaded area represents the swath coverage of the instrument or product; (b) the rain intensity in mm h^{-1} are represented according to the color scale included in the figure, from 0 to 35 mm h^{-1}; (c) the first column (panels a, c, e, g, and i) refers to 0030 UTC and the second (panels b, d, f, h, and j) to 0100 UTC; (d) the town of Algiers is marked by a red circle.

The inspection of PMW rain maps (panels a and b) reveals that coastal precipitation is missed altogether. Starting 50 km offshore and coming ashore the NESDIS algorithm uses the land module, i.e., precipitation in coastal environment is treated as it were over land. This is the most difficult zone to treat because of the discontinuity in atmospheric conditions and of the mixed sea-land signal collected within the field of view. In order to try to explain the complete lack of precipitation signal along the coast, the NESDIS algorithm was modified to eliminate the ad hoc treatment of coastal environment: overseas pixels were processed by means of the “sea” algorithm and overland with the “land” algorithm, no matter how far from the coast. The result somewhat unexpected of this exercise is that the “sea” part of the PMW algorithm works fairly well and detects convective cells along the coast, although at reduced rain intensity. Nonetheless, spurious rain signatures appear all along the coast even in cloud free conditions. On the contrary, no relevant rain signatures appeared inshore. It is thus evident that the “land” part of the algorithm is completely unfit for the particular rain type and/or surface characteristics. By analyzing the terrain classification applied prior to the rain computation it appears that some small (precipitation?) area is misclassified as snow. The largest part of precipitation over the Mediterranean sea is derived by means of the scattering algorithm. The heaviest precipitation is detected over the Mediterranean off the coast of North Africa, and the values never exceeded 13 mm h^{-1}. Because of the lack of SSM/I overpasses after 1958 UTC (the successive orbit is at 0504 UTC the day after) the relationships derived from the two orbits are used to derive the rainfall maps during the night. Heavy rain started falling after this overpass, so that the algorithm faced very critical data input conditions.

The analysis of the NRLT results for the same time period (b and d) do not bring about substantial improvements with respect to PMW’s. Almost no precipitation is detected over the African continent, excluding light rain over the Algeria-Tunisia border. One of the most prominent merit of the hybrid method is that it *can* eliminate discontinuities and mitigate the problem of directly deriving precipitation over the coast from PMW, but in this case even this type of technique is of no avail in detecting precipitation over Algiers.

The geolocated statistical RR-T_B relationships for the nine boxes covering the area show that the heaviest precipitation appear to be associated with the Algiers box and the one immediately to the North, with a maximum intensity of about 9 mm h^{-1}. The adjacent boxes show similar relationships, but with a reduced rain intensity. The zero-rain threshold is always < –40°C (–47°C for the box containing Algiers), and the range of temperatures associated to precipitation is no more than 10°C if one considers intensities >1 mm h^{-1}. These relationships are obviously derived from rainy pixels over the sea. Since the NRLT is based in the end on the IR T_B, METEOSAT IR images for the whole night were analyzed, considering a 1°×1° box centered over Algiers. The T_Bs remained constantly higher than the zero rain threshold, and this explains why no precipitation is detected. In practice the behavior of the NRLT in the particular case reveals that the characteristics of the clouds and precipitation fields were definitely different over land (warm rain) with respect to the convective cells embedded in the storm system, which developed over the sea very close to the coastline. This is confirmed by the PR observations (panels e and f) that show very intense precipitation cells off the Morocco-Algeria coast that appear to be delimitated by the coastline. Very likely the orography played a major role in the event, especially the relief south of Algiers, giving rise to a precipitating system that, although embedded in a larger field, was neither detected by PMW (due to the low scattering) nor by the NRLT (due to the high T_B).

The NRLT was further calibrated using PR rain measurements. The results (panels g and h), however, look quite disappointing. The rain pattern is not much different with respect to panels c and d, but the rain intensity values rose to much higher values, according to the radar measurements. Indeed the PR data, due to very narrow swath of the instrument, drastically change only the relationships of the westernmost boxes, altering the rain intensity associated with each IR temperature, but not the overall shape of the relationship. Unfortunately, due to the low number of overpasses and the characteristics of the TRMM orbit, the PR did not take measurements over the area of the disaster.

For comparison with the NRLT results TMI rainfall maps are shown in panels i and j. The maps reveal that most of the precipitation over Algiers is missed, even if the TMI rain product is derived by means of a completely different PMW algorithm, the Goddard Profiling Algorithm (GPROF; Kummerow et al. 2001; McCollum and Ferraro 2003). In general, quite low precipitation is detected over the land. Rain rates do not differ very much between the two methods, but are in general lower for NRLT. In the NRLT maps the rain field appears shifted to the North, preventing a meaningful numerical comparison between the two, but the main features of the field seem fairly preserved, even 4 h after the calibration.

5 CONCLUSIONS

Tests of a global blended PMW-IR satellite rainfall technique were conducted for two rainfall events in the Mediterranean area: (1) rainstorms over the Po Valley in Northern Italy and (2) a coastal heavy, flood-producing storm over Algiers. The technique constantly evolves in time due to the ever-expanding suite of PMW sensors and multispectral GEO imagers. However crude the blending mechanism might be, as for instance in the use of a single thermal IR channel, the technique performed fairly well when the underlying MW algorithm supplies reliable input rain maps for its calibration.

Results show that, on one hand, the technique suffers from the usual shortcomings of the adopted PMW algorithm, as for instance the unsatisfactory treatment of coastal environments and the possible misclassification of pixels in the screening procedure that precedes the rain retrieval. In certain environments these deficiencies prevent rainfall detection in the first place and therefore a complete representation of precipitation fields, as demonstrated by the analysis of the Algeria event. Moreover, the technique reveals intrinsic shortcomings connected mainly to the presence over the same area of quite different precipitation types, as is the case of very cold convective nuclei embedded in stratiform fields. The technique establishes geolocated rainrate/brightness temperature relationships that are the more correct the more homogeneous the characteristics of the precipitation field for the analysis area. This is obviously driven by the global design of the technique.

On the other hand, if the previous unfavorable conditions do not arise, the technique is able to fairly reconstruct the precipitation field outside the space/ time domain covered by PMW observations, even in case of sparse and uneven PMW overpasses. The improvement of PMW rain estimations and the use of multispectral channel analysis will add more precision to the presently available blended products.

It is conceivable that the advent of the ongoing international missions aimed to dramatically reduce the gaps between successive MW observations does not undermine the usefulness of blended techniques that remain the preferable method for producing reliable instantaneous rainfall maps, if they are required to be global, frequent and continuous in space.

6 REFERENCES

Adler, R. F., C. Kidd, G. Petty, M. Morrissey, and H. M. Goodman, 2001: Intercomparison of global precipitation products: The third precipitation intercomparison project (PIP-3). *Bull. Amer. Meteor. Soc.*, **82**, 1377–1396.

Calheiros, R. V. and I. Zawadzki, 1987: Reflectivity rain-rate relationship for radar hydrology and Brazil. *J. Climate Appl. Meteor.*, **26**, 118–132.

Ferraro, R. R., 1997: Special sensor microwave imager derived global rainfall estimates for climatological applications. *J. Geophys. Res.*, **102** (D14), 16715–16735.

Ferraro, R. R. and G. F. Marks, 1995: The development of SSM/I rain-rate retrieval algorithms using ground-based radar measurements. *J. Atmos. Oceanic Technol.,* **12,** 755–770.

Kummerow, C., Y. Hong, W. S. Olson, S. Yang, R. F. Adler, J. McCollum, R. Ferraro, G. Petty, and T. T. Wilheit, 2001: The evolution of the Goddard Profiling Algorithm (GPROF) for rainfall estimation from passive microwave sensors. *J. Appl. Meteor.*, **40**, 1801–1820.

Turk, F. J., G. Rohaly, J. Hawkins, E. A. Smith, F. S. Marzano, A. Mugnai, and V. Levizzani, 2000a: Meteorological applications of precipitation estimation from combined SSM/I, TRMM and geostationary satellite data. *Microwave Radiometry and Remote Sensing of the Earth's Surface and Atmosphere*, P. Pampaloni and S. Paloscia, eds., VSP, Utrecht, The Netherlands, pp. 353–363.

Turk, F. J., G. Rohaly, J. Hawkins, E. A. Smith, F. S. Marzano, A. Mugnai, and V. Levizzani, 2000b: Analysis and assimilation of rainfall from blended SSMI, TRMM and geostationary satellite data. *Proc. 10th AMS Conf. Sat. Meteor. Ocean.*, 9–14 January, Long Beach, CA., 66–69.